



4-1986

Medium Modified Proton Densities Deduced from Electron Scattering Experiments

Steven Paul DeRyke
Western Michigan University

Follow this and additional works at: https://scholarworks.wmich.edu/masters_theses



Part of the Nuclear Commons

Recommended Citation

DeRyke, Steven Paul, "Medium Modified Proton Densities Deduced from Electron Scattering Experiments" (1986). *Masters Theses*. 1295.

https://scholarworks.wmich.edu/masters_theses/1295

This Masters Thesis-Open Access is brought to you for free and open access by the Graduate College at ScholarWorks at WMU. It has been accepted for inclusion in Masters Theses by an authorized administrator of ScholarWorks at WMU. For more information, please contact wmu-scholarworks@wmich.edu.



**MEDIUM MODIFIED PROTON DENSITIES
DEDUCED FROM ELECTRON
SCATTERING EXPERIMENTS**

by

Steven Paul DeRyke

**A Thesis
Submitted to The
Faculty of The Graduate College
in partial fulfillment of the
requirements for the
Degree of Master of Arts
Department of Physics**

**Western Michigan University
Kalamazoo, Michigan
April 1986**

MEDIUM MODIFIED PROTON DENSITIES
DEDUCED FROM ELECTRON
SCATTERING EXPERIMENTS

Steven Paul DeRyke, M.A.

Western Michigan University, 1986

Recently two fundamental problems in nuclear physics have been resolved by applying the concept of nucleon size increases over that of free nucleons. These successes have encouraged the use of medium-modified proton densities to explain the differences between Hartree-Fock calculations and experimental charge densities. These differences constituted a long standing problem in nuclear physics.

The covariant soliton model of density dependent nucleon form factors was employed to explain these differences. This model predicts a non-linear relationship between point proton densities and charge densities. This work was able to provide a self-consistent proton density for ^{208}Pb by inverting this relationship. The final form of the proton density provides an excellent quantitative agreement with accepted Hartree-Fock calculations.

ACKNOWLEDGEMENTS

The execution and completion of this work was made not only possible, but thoroughly enjoyable through association with my research adviser, Dr. Al Rosenthal. I wish to thank him for allowing me many professional opportunities and experiences in representing my own research not ordinarily granted to a Master's degree candidate.

I am indebted to Dr. Dean Halderson, and Dr. Mark Clark for their contributions to the technical aspects of this project. I would like to thank Dr. Robert Shamu for the part he played as one of my thesis committee members.

This work would not have been accomplished without the continual support of my wife, Cindy, given freely in spite of the demands of her own professional career. I also wish to thank my mother, for her love and great expectations.

Steven Paul DeRyke

INFORMATION TO USERS

This reproduction was made from a copy of a document sent to us for microfilming. While the most advanced technology has been used to photograph and reproduce this document, the quality of the reproduction is heavily dependent upon the quality of the material submitted.

The following explanation of techniques is provided to help clarify markings or notations which may appear on this reproduction.

1. The sign or "target" for pages apparently lacking from the document photographed is "Missing Page(s)". If it was possible to obtain the missing page(s) or section, they are spliced into the film along with adjacent pages. This may have necessitated cutting through an image and duplicating adjacent pages to assure complete continuity.
2. When an image on the film is obliterated with a round black mark, it is an indication of either blurred copy because of movement during exposure, duplicate copy, or copyrighted materials that should not have been filmed. For blurred pages, a good image of the page can be found in the adjacent frame. If copyrighted materials were deleted, a target note will appear listing the pages in the adjacent frame.
3. When a map, drawing or chart, etc., is part of the material being photographed, a definite method of "sectioning" the material has been followed. It is customary to begin filming at the upper left hand corner of a large sheet and to continue from left to right in equal sections with small overlaps. If necessary, sectioning is continued again—beginning below the first row and continuing on until complete.
4. For illustrations that cannot be satisfactorily reproduced by xerographic means, photographic prints can be purchased at additional cost and inserted into your xerographic copy. These prints are available upon request from the Dissertations Customer Services Department.
5. Some pages in any document may have indistinct print. In all cases the best available copy has been filmed.

**University
Microfilms
International**

300 N. Zeeb Road
Ann Arbor, MI 48106

1328108

DeRyke, Steven Paul

MEDIUM MODIFIED PROTON DENSITIES DEDUCED FROM ELECTRON
SCATTERING EXPERIMENTS

Western Michigan University

M.A. 1986

University
Microfilms
International 300 N. Zeeb Road, Ann Arbor, MI 48106

TABLE OF CONTENTS

ACKNOWLEDGEMENTS	ii
LIST OF TABLES AND FIGURES	iv
CHAPTER	
I. INTRODUCTION	1
Quark Models	1
EMC Effect	3
Longitudinal Response Function	4
II. CHARGE AND MATTER DISTRIBUTION OF ^{208}Pb	7
Modification of Nucleon Properties	7
Shell Model Calculations	12
Relation of Charge and Matter Densities	14
III. NUMERICAL TECHNIQUES	18
Density Forms	18
Minimization Techniques	19
IV. RESULTS AND DISCUSSION	22
Results	22
Future Research	24
Conclusions	26
BIBLIOGRAPHY	28

LIST OF TABLES

1. Calculated and Experimental Nucleon Properties . 9
2. Proton Form Factors and the Nuclear Matter to
Free Space Ratios 10
3. Neutron Form Factors and the Nuclear Matter to
Free Space Ratios 11

LIST OF FIGURES

1. CSM Feynman Diagram	2
2. Ratio of Nuclear Structure Functions Per Nucleon	4
3. Longitudinal Response Function	5
4. Proton Electric Form Factors in Free Space and in Nuclear Matter	7
5. Proton Magnetic Form Factors in Free Space and in Nuclear Matter	7
6. Quark Wave Functions	8
7. Charge Densities	13
8. Charge Densities and RPA Corrections	15
9. Standard Model Proton Densities	23
10. Flat Matter Proton Density	24

CHAPTER I

INTRODUCTION

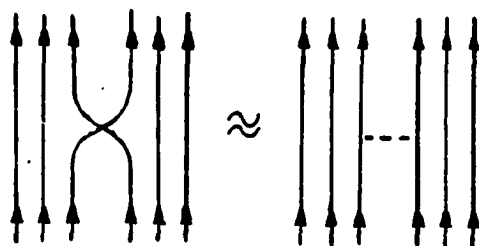
Quark Models

The existence of quarks in nuclei was firmly established through the theory's ability to explain Bjorken scaling of deep inelastic scattering experiments. High energy leptons did not behave as if they were being inelastically scattered from individual nucleons. Instead, the appearance was one of elastic scattering with some component particles of the nucleon. Analysis of this quasi-elastic scattering data described a point-like particle with spin $1/2$ and charge of absolute value $1/3$ or $2/3$. Since then, several quark models have been devised which attempt descriptions of nucleon and/or bulk nuclear properties. These models include potential and bag models which can be characterized by their confinement description, as well as the covariant soliton model, or CSM, that is the focus here.

The CSM is not a fundamental theory but a phenomenological model developed to provide an accurate, yet workable interpretation of experiment. To achieve this, the development was motivated by quantum

chromodynamics, or QCD. Unfortunately, QCD is currently unsolvable; therefore, to remain workable, the CSM includes only those degrees of freedom that are appropriate to nuclear physics. Two features of QCD, mesons and quarks, are included in a relativistic field theory. These satisfy three primary requirements: to give the correct force between nucleons, explain the binding of quarks without gluons, and allow for nucleon motion without the need for explicit recoil corrections.

Gluons are not considered an appropriate degree of freedom, since nucleons are not sensitive to the color force. However, the binding force between nucleons can be well described by meson exchange. Within the CSM, quarks as constituents of the nucleon are the particles that actually exchange these mesons (Fig. 1). This naturally leads to the approximation that the exchange of mesons between quarks in the same nucleon can, with minor corrections, describe the binding.



(a) Quark Exchange (b) Meson Exchange

Figure 1. The QCD View of Nucleon Binding Based on Quark Exchange and the Equivalent CSM View Based on Meson Exchange.

EMC Effect

The European Muon Collaboration, or EMC, study of deep inelastic lepton scattering revealed that the ratios of structure function per nucleon were mass number dependent (Fig. 2).. These results indicate a distinct redistribution of quarks in nuclei as compared to a simple collection of nucleons with their free space distributions. There have been several attempts to remodel nucleons to predict this behavior, all involving an increase in the quark confinement volume. Of those the CSM appears to be the most complete. It achieves this completeness through the unification of relativistic nuclear structure dynamics, which has been highly successful in explaining a broad range of nuclear properties, and the quark models necessary to explain the EMC effect.

Reduction of the constituent quark mass through coupling to the ambient mesic field creates an additional Fermi pressure which leads to the expansion of the nucleon. This expansion, in turn, accounts for the enhanced scattering for Bjorken scaling, or $x < 0.3$ and suppressed scattering for $0.3 < x < 0.8$, where x is the Bjorken scaling factor. It is from this scattering data that the structure functions which identify the EMC effect can be derived. In this way, the CSM calculations

of the increase of nucleon size as a function of average nuclear density reproduce the values required to fit the mass-number dependence of the EMC effect to a remarkable degree.

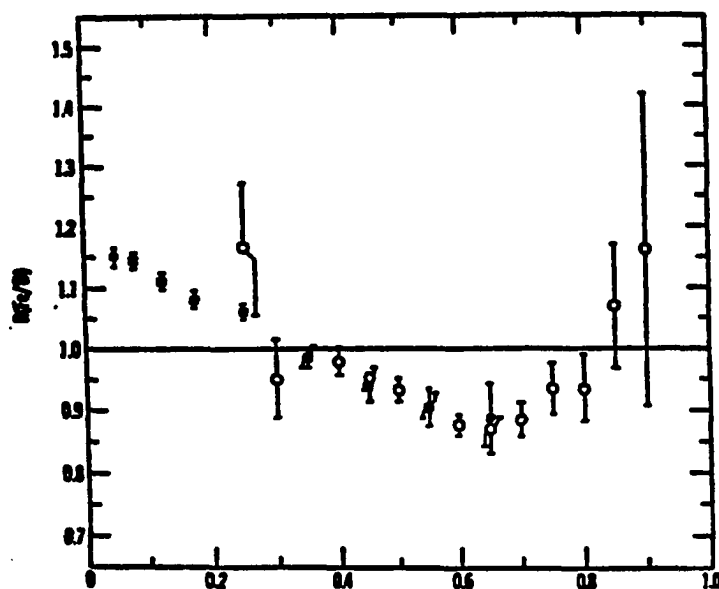


Figure 2. Experimental data for the ratio R of nuclear structure functions per nucleon as a function of average nuclear density. Data for iron and deuterium (Vary, 1984).

Longitudinal Response Function

Another problem in nuclear physics has been the inability of impulse approximations to correctly predict the quenching of longitudinal response functions for deep inelastic electron scattering. A modification in the form of increased nucleon size that could account for this difference was first put forward by Noble (1980). The mechanism responsible for the increase was left for later speculation.

Due to its density dependent nature, the CSM is able to predict this reduction in the energy distribution of the scattered electrons (Fig. 3). One picture is that the increase in quark confinement volume leads to a stiffening of the electromagnetic nucleon form factors. However, it is more easily viewed as the CSM quark wave functions directly generating reduced form factors. As Fourier transforms of the charge densities, these form factors are responsible for the scattering behavior of charged particles. This modification accurately predicts the experimentally verified reduction of flux near the nucleon quasi-elastic peak.

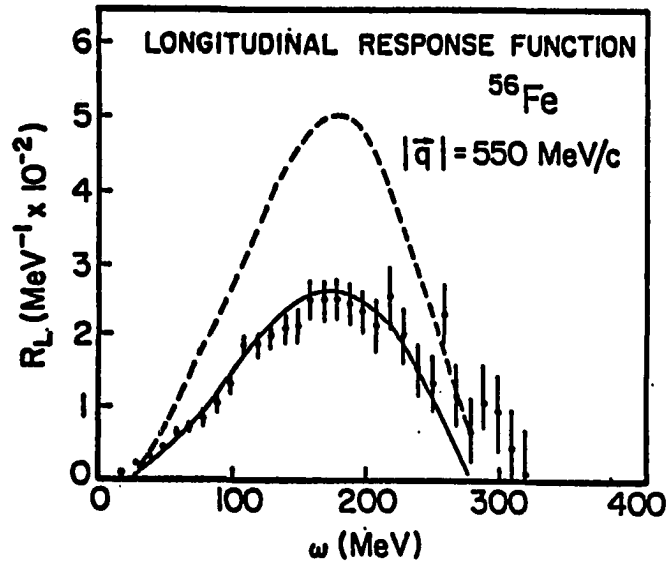


Figure 3. Calculated Longitudinal Response Function based on unmodified form factors (dashed) and CSM modified form factors (solid) compared to data (Celenza, Harindranath, Shakin and Rosenthal, 1984).

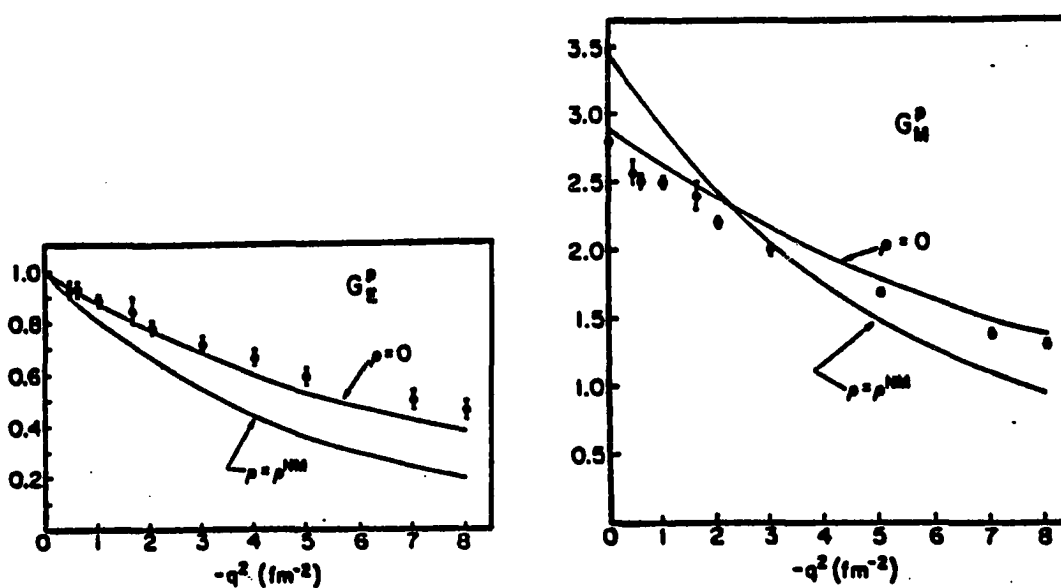
These successes of the CSM have been the source of encouragement in application of this model to related areas of nuclear physics. One such area has been the difference between Hartree-Fock shell model calculations and experimental charge densities. It is this problem that will be addressed in this thesis.

CHAPTER II

CHARGE AND MATTER DISTRIBUTION OF ^{208}Pb

Modification of Nucleon Properties

As previously seen, a physical mechanism for the increase in nucleon size exists in the interaction of the quarks with the ambient mesic field. But a more rigorous discussion must be based on modified nucleon properties (Fig. 4 and 5) that can be generated directly from the model (Celenza, Harindranath, Rosenthal and Shakin, 1985).



Figures 4. and 5. Calculated electric and magnetic form factors in free space and nuclear matter for protons (Celenza, Rosenthal and Shakin, 1984).

These modifications arise from calculations in terms of the quark wave functions (Fig. 6) or the nucleon-diquark amplitudes.

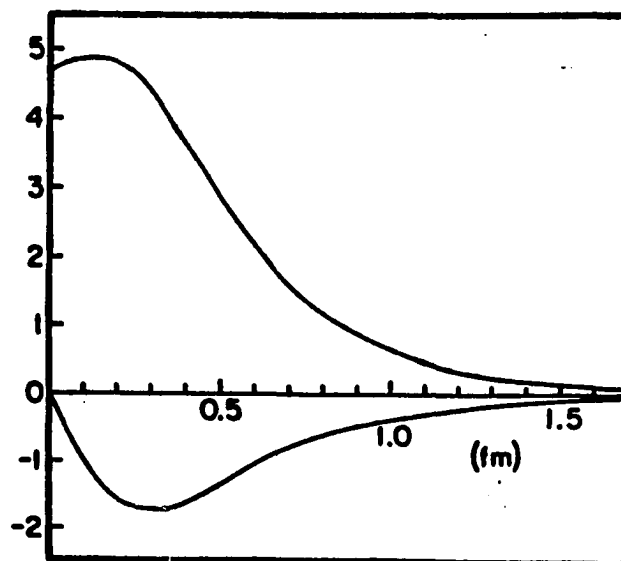


Figure 6. Coordinate-space quark wave functions obtained by Fourier transformation of the momentum-space amplitude in the nucleon rest frame. The curves represent the upper and lower radial components of the coordinate-space spinor (Celenza, Rosenthal and Shakin, 1984).

The basic success of these approximations can be seen in the modeling of key parameters for free nucleons, Table 1. Specifically, the model can accurately predict rms radii and coupling constants for both protons and neutrons in free space. Application of the model to nuclei is accomplished by using a local density approximation that the matter inside a nucleus

Table 1
Calculated and Experimental Nucleon Properties

	Calculated	Experimental
Baryon density rms radius	0.647 fm	
Scalar density rms radius	0.511 fm	
$\epsilon = m_N - \langle E_d \rangle$	181 MeV	
$\langle E_d \rangle$	1314 MeV	
m_N	1495 MeV	
\mathcal{E}_s	205 MeV	
\mathcal{E}_v	168 MeV	
\mathcal{E}_a	-133 MeV	
\mathcal{E}_p	29 MeV	
\mathcal{E}_x	528 MeV	
m_{NN}	1342 MeV	938 MeV (1087 MeV) ^a
$\langle r_p^2 \rangle_E^{1/2}$	0.867 fm	0.87 ± 0.02 fm ^a
$\langle r_p^2 \rangle_N^{1/2}$	0.813 fm	0.80 ± 0.03 fm ^a
$\langle r_n^2 \rangle_N^{1/2}$	0.820 fm	0.79 ± 0.15 fm ^a
$-\left[\frac{dG_E^N(q^2)}{dq^2} \right]$	3.65×10^{-2} fm ²	$(1.89 \pm 0.04) \times 10^{-2}$ fm ²
μ_p	2.76	2.79
μ_n	-1.81	-1.91
μ_p/μ_n	1.50	1.46
g_A	1.27	1.25
$g_s = \frac{G_{sNN}}{\rho_s(0)}$	$\frac{7.63}{1.94} = 3.93$	
$g_s = \frac{G_{sNN}}{g_1(0)}$	$\frac{12.91}{4.78} = 2.70$	
$g_a = \frac{G_{aNN}}{3}$	$\frac{13.3}{3} = 4.43$	
$g_p = \frac{G_{pNN}}{1}$	$\frac{4.34}{1} = 4.34$	
$\frac{G_p^T}{G_p^V} = \frac{F_{21}(0)}{F_{11}(0)}$	3.56	3.50 ^b
$\frac{G_a^T}{G_a^V} = \frac{F_{20}(0)}{F_{10}(0)}$	-0.048	0.0 ^b

can be modeled by infinite nuclear matter of equal density. Properties of nucleons in this type of environment are more interesting because of their effect on nuclear properties. Calculations of the Sachs form factors (Tables 2 and 3) reveal the density dependence so crucial to the model's ability to explain experiment. It is to these properties and the manners in which they are modified that further comparison to experiment must be done.

Table 2

Proton Form Factor and Nuclear Matter to Free
Space Ratios (Celenza, Rosenthal
and Shakin, 1984)

$-q^2$ (fm ⁻²)	$G_M^p(q^2, 0)$	$\frac{G_M^p(q^2, \frac{1}{3})}{G_M^p(q^2, 0)}$	$\frac{G_M^p(q^2, \frac{2}{3})}{G_M^p(q^2, 0)}$	$\frac{G_M^p(q^2, 1)}{G_M^p(q^2, 0)}$
0	2.90	1.05	1.11	1.19
1	2.62	1.03	1.07	1.10
2	2.39	1.02	1.03	1.02
3	2.16	1.00	0.99	0.95
4	1.97	0.99	0.95	0.88
5	1.79	0.97	0.92	0.82
6	1.64	0.96	0.89	0.78
7	1.50	0.95	0.87	0.74
8	1.38	0.94	0.84	0.71

Table 3

Neutron Form Factor and Nuclear Matter to Free
Space Ratios (Celenza, Rosenthal
and Shakin, 1984)

$-q^2$ (fm ⁻²)	$G_M^n(q^2, 0)$	$\frac{G_M^n(q^2, \frac{1}{3})}{G_M^n(q^2, 0)}$	$\frac{G_M^n(q^2, \frac{2}{3})}{G_M^n(q^2, 0)}$	$\frac{G_M^n(q^2, 1)}{G_M^n(q^2, 0)}$
0	-1.90	1.05	1.12	1.20
1	-1.72	1.03	1.07	1.11
2	-1.56	1.02	1.03	1.03
3	-1.41	1.00	0.99	0.95
4	-1.29	0.99	0.96	0.89
5	-1.17	0.97	0.92	0.83
6	-1.07	0.96	0.89	0.77
7	-0.98	0.95	0.87	0.74
8	-0.90	0.94	0.85	0.71

Electron-nucleus scattering data is conventionally interpreted in terms of constituent nucleons whose interactions with the electromagnetic field are unmodified from their free space form. In practical terms, one deduces a matter form factor by dividing the experimental charge form factor by the free space nucleon electromagnetic factor. The resulting matter form factor F_m is said to be obtained by "unfolding the proton finite size". The term "impulse approximation" is used to describe the practice of substituting the free space t-matrix for the "in the medium" t-matrix in a

scattering calculation. Because of its similarity to this procedure, we have chosen to call the approximation, represented by Eq. 1, the "impulse approximation". This work can be regarded as identifying corrections to that approximation.

$$\rho_{\text{chg}}(r) = \frac{2}{\pi} \int q^2 j_0(qr) dq G_E(q^2) \int r'^2 j_0(qr') \rho(r') dr'$$

Shell Model Calculations

The Hartree-Fock shell model has long been one of the most useful methods for calculating the ground state of a system of interacting fermions. However, charge densities generated from the calculated matter densities do not successfully compare with experimental charge densities. Theoretical charge densities based on the impulse approximation show only the slightest trend toward the correct values for large nuclei. The fact that these theories were more successful for light nuclei points directly to some form of density dependence, and therefore, a logical application of CSM.

Hartree-Fock-Bogolyubov, or HFB, calculations done by Decharge and Gogny (1980) show a pronounced peak near the nuclear center for the matter density; however, a plot of the experimental charge density remains relatively flat in this same area (Fig. 7).

Alternatively, work by Negele and Vautherin (1972) predicts a depletion of S-state protons in the central region based on calculations of pairing interactions. This pairing force between protons and outer shell neutrons causes the respective densities to oscillate out of phase thus generating a net matter density that is flat.

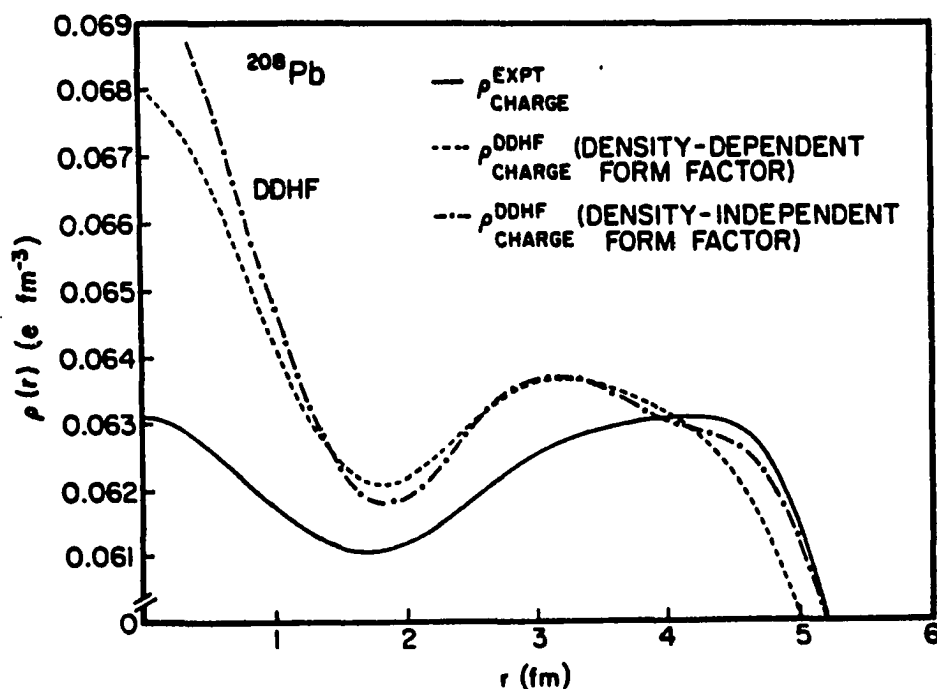


Figure 7. Comparison of Calculated and Experimental Charge Densities (Celenza, Harindranath, Rosenthal and Shakin, 1985).

These theories represent the two extremes in proton and neutron density relationships. This relationship enters directly into the density dependent form factors of the CSM and therefore, effects the generated charge densities. Application of the CSM to both cases will

thus provide a range within which the true proton density must lie.

The explanation applied to the longitudinal structure function problem can be viewed here as a reduction in the central charge concentration as the nucleons expand. Therefore, although the point proton density is higher in the center, the charge is spread enough so its density remains basically uniform out to the surface. To test a model's ability to correctly describe this effect, it is necessary to be able to produce one set of values, either the matter or charge density, when provided with the other.

Relation of Charge and Matter Densities

An earlier work (Celenza, Harindranath, Rosenthal and Shakin, 1985) was in this respect a partial success. It showed a definite trend toward agreement with experimental charge densities when applying the CSM to the Hartree-Fock matter density. Later inclusion of effects attributed to random phase approximation, or RPA, corrections improved their agreement significantly and demonstrated a clear superiority over impulse approximation results (Fig. 8). These results were not completely satisfactory, in that they did not provide the actual form of the matter density. It is the intent

of this work to provide such a form.

The conceptual basis for generating a specific form for the density comes from work by Sick (1973) that progressed in the following way. Form factors with uncertainties of less than a few percent were generated from elastic electron scattering experiments at Centre d'Etudes Nucleaires de Saclay, France. The charge densities extracted from this data were then used to derive a unique form for the proton density using a sum of twelve Gaussians. Since this work was done in impulse approximation the double fourier transform was just a linear integral equation and a good fit was obtained by varying only the heights of the Gaussians. The simplicity of this problem allowed the use of a gradient search method and led to rapid convergence.

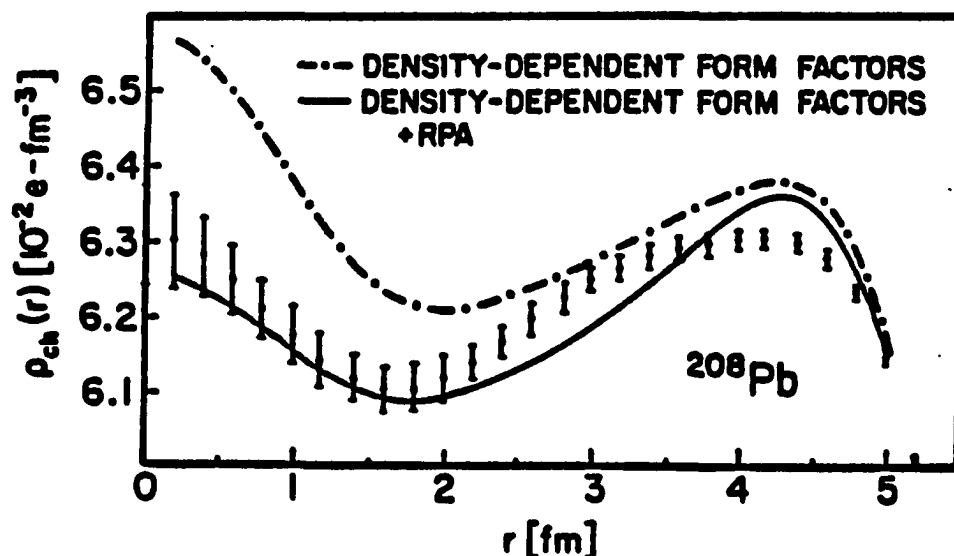


Figure 8. Charge Densities and RPA Corrections (Celenza, Harindranath, Shakin and Rosenthal, 1985).

Charge and matter densities are related through a double Fourier transform (Eq. 2), and the manner of density dependence in the CSM makes this a non-linear integral equation. Solutions to this type of equation are extremely difficult to generate in analytic form. However, satisfactory results were obtainable through numerical analysis of this double Fourier transform once nucleon form factors were available.

$$\rho_{\text{chg}}(\mathbf{r}) = \frac{2}{\pi} \int q^2 j_0(q\mathbf{r}) d\mathbf{q} \int \mathbf{r}'^2 j_0(q\mathbf{r}') G_E(q^2, \rho(\mathbf{r}')) \rho(\mathbf{r}') d\mathbf{r}'$$

Solution of the many body problem for three quarks per nucleon in a system of 208 nucleons is impossible at this time. Any attempt within the system to derive quark wave functions from which nuclear form factors could be produced cannot hope to succeed. However, by generalizing to an infinite body problem, a set of wave functions and related nucleon form factors can be solved. These will be density dependent and a complete range of values can be produced for use with many varied nuclei. By fitting to these values, an analytic form of these form factors was produced for use in the numerical analysis.

This local density approximation allows the generation of nuclear form factors based on the nucleon

form factors appropriate to infinite nuclear matter of the applicable density. It is from these nuclear form factors that charge densities can be calculated for comparison to experimental results.

CHAPTER III

NUMERICAL TECHNIQUES

Density Forms

By assuming a form for the unknown proton density an iterative approach to solving the non-linear integral equation (Eq. 2) was possible. Variation of the parameters in the assumed form can then be used to produce new charge densities. Comparison of these to the correct charge density allows a trial and error approach in adjusting the parameters to give the correct proton density.

The charge density used as data in this procedure was itself a result of calculations. The nuclear form factors produced at Saclay required radiative corrections before they could be used to generate the charge density needed above.

Based on a concept used by Sick (1973), the proton density was modeled by a sum of twelve Gaussians (Eq. 3). The heights Q_i and positions R_i of these Gaussians provided an adequate number of free parameters to correctly match the variations in charge density.

$$\rho_p(x) = \frac{Z}{2\pi^{3/2}\gamma^3} \sum_{i=1}^{12} \frac{Q_i}{1+2R_i^2/\gamma^2} \left[e^{-(x-R_i)^2/\gamma^2} + e^{-(x+R_i)^2/\gamma^2} \right]$$

Double Fourier Transformation

The relationship between the charge and proton densities is expressed through a double integral. In the impulse approximation, the proton density only enters through one term, the density. The density dependent version of the equation has an additional term that includes the density, the nucleon form factor. This term represents the non-linear aspect of the integral equation and provides the main difficulty in finding a solution.

Considerations of speed and accuracy led naturally to the use of a Gaussian integration routine. The specific subroutine employed 96 points over the range of integration, guaranteeing complete coverage of any oscillations. Center of weighting for these points was determined by comparison of tests cases against a Newton-Cotes routine that had adjustable accuracy. Use of this other routine, during the minimization procedure, was impractical due to its high computational time requirement.

Minimization Technique

In the present work minimization was achieved through the use of a random walk algorithm developed by

Hooke and Jeeves (1961). Initial values were allowed to vary by a chosen step size until an improvement could no longer be found. The step size was then reduced and values were again varied. Searching continued until a predetermined minimum step size was reached.

Gradient type of searches are arguably faster, but the instability of the problem could have led to incorrect results. Indeed, instabilities of this type prevented successful completion of the original investigation at Brooklyn College. Additionally, the subroutine used was designed to take advantage of the special strengths of computing machines. Specifically, that gradients in this type of problem are very complex and solving for them could expend more machine time than they save.

Direct minimization of the differences between corresponding values of data and calculated charge densities tends to consider high q^2 (or low r) values too highly. A weighted comparison was therefore necessary to avoid using data regardless of its relative accuracy. Use of a chi-squared fit in the minimization allowed the program to work hardest in those areas known best. Specifically, a good fit to the surface region was most important. Final acceptance of the associated parameters was based on the calculated charge density

being closer to experimental values than Sick's own work which varied only the twelve Gaussian heights. This comparison was done by hand after each machine run had stopped at a predetermined step size.

CHAPTER IV

RESULTS AND DISCUSSION

Results

Modeling of the charge density through the method previously discussed was so successful that no distinction between calculated and experimental values (dotted) is evident graphically (Fig. 9). The true success of this work though, lies in the similarity of the generated proton density (solid) and the HFB calculation of DeCharge and Gogny (dashed). Both curves contain three oscillations with only minor phasing differences. There is a definite qualitative agreement in the important surface region ($r > 6$ fermi). It is clear that medium modified nucleon sizes can correct for a major portion of the failure to match charge densities when applying standard forms of shell model theory.

The quantitative disagreement between HFB and the matter densities generated in this work for values of $r < 6$ fermi were expected for two reasons. First, the HFB calculations do not include ground state corrections similar to the RPA previously discussed (though these corrections could very well increase the disagreement).

Secondly, a local density approximation contained in the CSM must certainly contribute to the disagreement, especially since the accuracy of the approximation is dependent on the rate of change of the density. This causes an increase in the size of the peak with increasing slope.

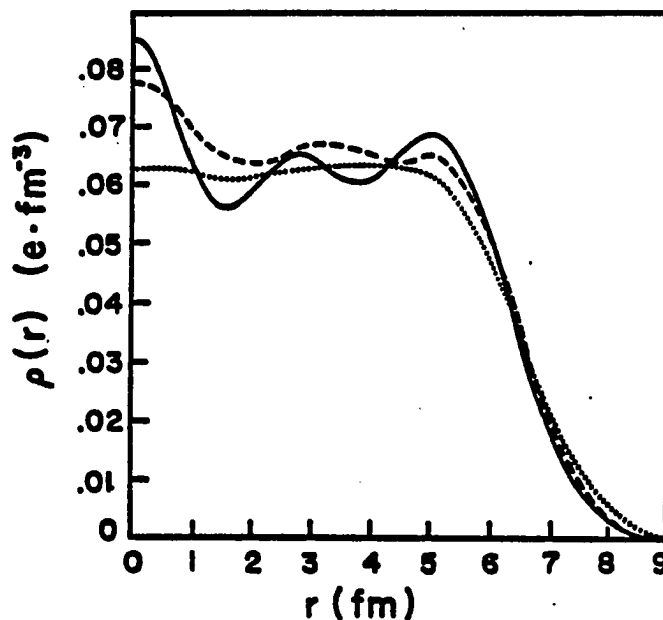


Figure 9. Standard Model Proton Densities (DeRyke and Rosenthal, 1986).

The numerical analysis was repeated assuming a simple Fermi form for the matter density, similar to Negele's model. Again, an excellent match to charge density was achieved (Fig. 10 dotted), and the resulting proton density (solid) modeled qualitatively the HFB calculations (dashed).

Direct comparison of the generated and HFB proton densities again reveals agreement in three key areas.

All three of the shell model peaks were predicted, the phasing of those peaks is correct and there is excellent agreement near the surface. In both cases, most notable is the presence of the large central peak while still being compatible with a flat charge density. No other theory or model has been able to provide this link between the highly regarded shell model calculations and the widely reproducible experimental results.

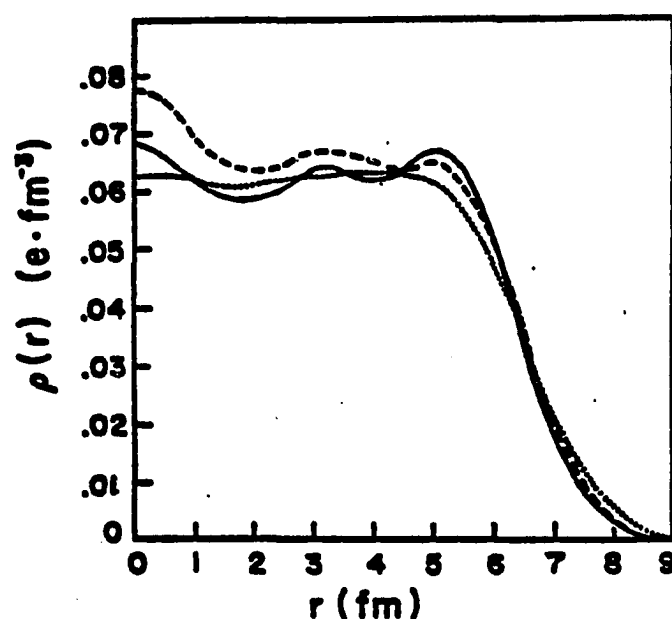


Figure 10. Flat Matter Proton Density

Future Research

The qualitative agreement achieved in this research must certainly be viewed as a success. So much so, in fact, that we believe future work in shell model calculations should not have their free parameters fit

to charge densities without this correction. However, more work is necessary before a truly quantitative agreement can result. Until a solution to QCD is available, improvement must come through refinement of the approximations in the model.

Two areas that seem most likely to leave behind a workable model once solved for exactly are the refinement of the local density approximation and the inclusion of neutron form factors. These corrections represent the direction which future work within this model should take, but valuable progress can also be derived from improvements in shell model calculations. Specifically, clarification of the strength of pairing interactions between protons and neutrons could determine the correct phasing of the associated densities. However, further tests do not have to wait for the improvements to these approximations.

Similar results from other nuclei would be valuable in determining the strength of this effect over a range of nuclear sizes and densities. Work of this type is currently underway by the author based on experimental data for ^{39}K , ^{40}Ca , ^{48}Ca and ^{20}Si .

Another area of concern open to the present research is the disagreement between scattering results of leptons and hadrons from light nuclei. A successful

accounting of these differences through medium modified nucleon sizes would be an important verification of the model.

Although the concept of medium modified densities is not yet generally accepted, it provides a unified explanation of three disparate and otherwise unexplained nuclear phenomena. Yet it is both workable and provides a reasonable physical view. Whatever the results from future research, the CSM has provided in its description a goal for other models and theories.

Conclusions

The ability of the model studied in this work to describe the experiments cited has lent credence to the existence of a density dependence of nucleon properties. The question which this work has attempted to address is whether the correct relationship between matter and charge densities in nuclei can be generated by a model based on quark binding through meson exchange. If the relationship could be determined, then relatively low energy nuclear physics experiments might indeed be sensitive to nucleon structure. Therefore, since nucleon properties are important in many areas of high energy scattering research, study of the CSM could conceivably contribute to a more comprehensive understanding of the

nuclear force and related phenomena.

BIBLIOGRAPHY

Celenza, L.S., Harindranath, A., Rosenthal, A., & Shakin, C.M. (1985). Evidence for the modification of nucleon properties in nuclei from traditional nuclear physics experiments. Physical Review C, 31, 946-955.

Celenza, L.S., Harindranath, A., Shakin, C.M., & Rosenthal, A. (1985). Quark effects in the charge distribution of 208 Pb. Physical Review C, 31, 1944-45.

Celenza, L.S., Harindranath, A., Shakin, C.M., & Rosenthal, A. Quark effects in nuclear longitudinal response function. Unpublished.

Celenza, L.S., Rosenthal, A., & Shakin, C.M. (1984). Symmetry breaking, quark deconfinement, and deep inelastic electron scattering. Physical Review Letters, 53, 892-894.

Celenza, L.S., Rosenthal, A., & Shakin, C.M. (1985a). Covariant soliton dynamics: Structure of the nucleon. Physical Review C, 31, 212-231.

Celenza, L.S., Rosenthal, A., & Shakin, C.M. (1985b). Many-body soliton dynamics: Modification of nucleon properties in nuclei. Physical Review C, 31, 232-239.

Decharge, J., & Gogny, D. (1980). Hartree-Fock- Bogolyubov calculations with the D1 effective interaction on spherical nuclei. Physical Review C, 21, 1568-1593.

DeRyke, S., & Rosenthal, A. Nuclear medium dependence of proton structure and the charge density of 208Pb. Unpublished.

Hooke, R., & Jeever, T.A. (1961). Direct search solution of numerical and statistical problems. Journal of the Association for Computing Machinery, 8, 212-229.

Negele, J.W., & Vautherin, D. (1972). Density matrix expansion for an effective nuclear Hamiltonian. Physical Review C, 5, 1472-1493.

Nobel, J.V. (1980). Modification of the nucleon's properties in nuclear matter. Physical Review Letters, 46, 412-415.

Sick, I. (1973). Model-independent nuclear charge densities from elastic electron scattering. Nuclear Physics, A218, 509-541.

Vary, J.P. (1984). Quark distributions in nuclei: Results from lepton probes. Nuclear Physics, A418, 195c-214c.